LIMNOLOGY
and
OCEANOGRAPHY: METHODS

Limnol. Oceanogr.: Methods 11, 2013, 351–359

The effects of spatial and temporal variability at the sediment surface on aquatic eddy correlation flux measurements

Jennie E. Rheuban and Peter Berg*
Department of Environmental Sciences, University of Virginia, 291 McCormick Road, Charlottesville, VA 22904-4123, USA

Abstract

The eddy correlation technique has become a widely used approach to measure ecosystem scale fluxes in aquatic benthic environments; however, there are few theoretical studies designed to guide deployment planning, the characterization of flux variability, or how to correctly interpret measured fluxes. Here, a three-dimensional numerical model for the turbulent transport and mixing in the near-bottom water was used to examine how well variations in vertical flux due to heterogeneities in the benthic community are integrated in eddy correlation measurements. The results showed that an appropriate choice of measuring height above the sediment surface is crucial to obtain an accurate average of the vertical flux from heterogeneous benthic communities. Through regression analysis of modeling results, a set of simple analytical expressions were derived for this threshold measuring height as a function of two parameters: heterogeneity patch size and sediment surface roughness. The same model was also used to examine the time lag between when a change in vertical flux occurs at the sediment surface and when it reaches the measuring point. The results showed that this response time varies by several orders of magnitude depending on flow velocity, sediment surface roughness, and measuring height. Simple analytical expressions were also derived for the response time. Overall, the findings indicate that both the spatial variability in benthic communities and the response to temporal changes are important factors that should be considered in planning eddy correlation measurements and interpreting eddy correlation fluxes.

Eddy correlation (EC), sometimes termed eddy covariance, has been used since the early 1950s (Swinbank 1951) as an approach to measure fluxes of mass, energy, and momentum in the atmospheric boundary layer. The technique was recently modified for the aquatic environment by Berg et al. (2003) to measure fluxes of dissolved O_2 across the sediment-water interface, and has since been used in a wide variety of environments including riverine systems, permeable sediments, lake sediments, the deep oceans, arctic fjords, seagrass meadows, under ice sheets, the continental shelf, and coral reefs (Berg et al. 2003; Kuwae et al. 2006; Berg and Huettel 2008; Brand et al. 2008; McGinnis et al. 2008; Berg et al. 2009; Glud et al. 2010; Lorrai et al. 2010; Hume et al. 2011; Long et al. 2012; Reimers et al. 2012; Long et al. 2013; Berg et el. 2013). These sites included both uniform and heterogeneous benthic communities and EC measurements were made from a wide range of different measuring heights (8–80 cm). However, little information is given on why these heights were chosen or how different measuring heights may affect the flux.

The size and shape of the area that contributes to the flux, termed the 'footprint', of EC measurements was determined by Berg et al. (2007) through a three-dimensional (3D) numerical tracer modeling study. Berg et al. (2007) showed that whereas the footprint can be very large (50–100 m^2), the uneven distribution of the flux signal causes a large percentage of the signal to be from a smaller area within the footprint. As a result of this distribution, the maximum contribution to the flux signal typically arises from a location ~1 to 7 m upstream of the instrument depending on environmental conditions and measurement height (Berg et al. 2007). When EC is used to derive ecosystem-scale fluxes, this uneven distribution within the footprint may cause inaccurate interpretations of the measured fluxes when the benthic community is heterogeneous. For example, Fig. 1 illustrates a conceptual heterogeneous benthic community with patchy vegetated and unvegetated sediments. As the fluxes would vary across this

*Corresponding author: E-mail: jer4r@virginia.edu

Acknowledgments

Support for this study was provided by the University of Virginia and the National Science Foundation through grants from the Chemical Oceanography program (OCE-0536431 and OCE-1061364) and Division of Environmental Biology (DEB-0917696 and DEB-0621014).

DOI 10.4319/lom.2013.11.351

Fig. 1. Conceptual heterogeneous benthic community with theoretical eddy correlation footprints. Measuring points are given as a dot and flow is from left to right.

benthic community, it is important to understand if eddy correlation measurements taken in different locations (illustrated as different footprint ovals) would accurately represent the entire benthic ecosystem or if the fluxes measured may be skewed toward one component of the community or another depending on instrument placement. This is the first topic investigated in this study.

During EC deployments, physical drivers of production and respiration are often measured simultaneously (Glud et al. 2010; Hume et al. 2011; Long et al. 2012). For an accurate interpretation of the fluxes measured, it is also necessary to understand whether there may be any significant time lag between measurements of these controlling variables and the fluxes estimated with the EC instrument. The 90% response time is defined as the time lag between when a change in vertical flux occurs at the sediment surface and when it reaches the measuring point. This time lag has not yet been quantified, thus most previous studies using the EC technique have assumed an instantaneous response in measured fluxes with changes in the controlling variables. For example, the benthic O_2 flux may change rapidly as a result of varying light conditions at the sediment surface (e.g., Hume et al. 2011); however, this change in flux may take time to reach the measuring height and result in data inaccurately correlated in relationships. This is the second topic studied in this article. Our results complement a recent study by Holtappels et al. (2013) who showed that dynamic changes in mean water velocity and mean water column O_2 concentration can impact measured EC fluxes.

In summary, to further improve the interpretation of EC data, we have quantified the following characteristics of aquatic EC measurements: 1) the threshold measuring heights at which variability in fluxes due to heterogeneity in the benthic community is well integrated, and 2) the time lag between a change in flux at the sediment surface and its observation at the measuring height. From numerous simulations using a 3D numerical model for turbulent mixing of a tracer in the near bottom water, we derive simple correlations for these key characteristics. We finally present an example based on a previously published EC data using our correlations to estimate appropriate measuring heights and response times for a specific site.

Materials and procedures

Numerical solution

The numerical solution used in this study was adapted from Berg et al. (2007), who produced a detailed map of the footprint of the EC technique. The original model relies on a 3D mathematical formulation for the transport and dispersion of a conservative tracer in turbulent flow where separate parameterizations for the turbulent diffusion and molecular diffusion are used. As no analytical solution to this model exists, it is solved using a numerical control volume approach (Carnahan et al. 1969). The original model assumes that whereas turbulent diffusion and molecular diffusion contribute to mixing in the direction of the mean current, the x direction (Fig. 1), advection is significantly greater. Thus, downstream effects of fluxes from the benthic surface do not affect upstream conditions. This allows the 3D solution to be solved as a series of 2D solutions in the y-z direction (Fig. 1). At each time step, the solutions are produced using the "implicit alternating direction method" (Douglas 1955; Peaceman and Rachford 1955; Carnahan et al. 1969). To minimize the total number of calculations, symmetry in the x-z plane is used so that a solution is only found for $y \geq 0$. Also, to incorporate long footprints (e.g., 90 m along the x axis, Berg et al 2007), control volume sizes in the x-direction are significantly larger than that of the y-direction. Finally, to obtain a detailed description of vertical variation, a fine control volume size is used for the z-direction.

Heterogeneous fluxes

The original model for the analysis of the footprint (Berg et al. 2007) was altered to include the effect of benthic heterogeneities on EC flux measurements. The calculation domain was significantly reduced in both control volume size in the x and y directions (2 cm × 2 cm) and in total number of control volumes to minimize calculation times by using additional symmetry lines illustrated in Fig. 2A as dashed lines. The lower boundary condition was defined as a series of square patches to represent a heterogeneous benthic surface containing fluxes of different values (Fig. 2A). The upper boundary condition was given as a constant flux equal to the integration of the lower boundary condition. The upstream boundary con-

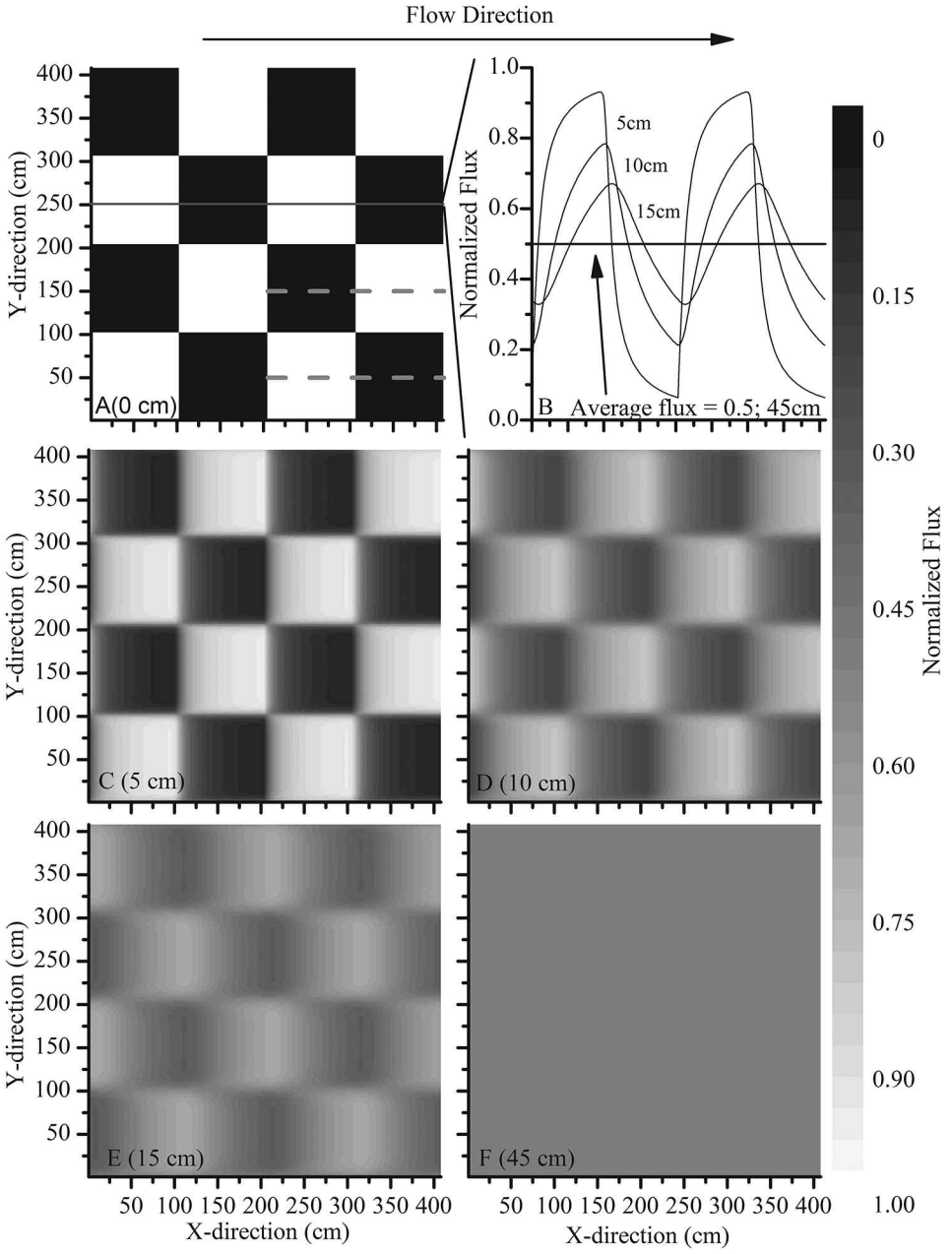

Fig. 2. (A) Checkerboard pattern of spatial flux heterogeneity on the sediment surface as seen from above. Flow direction is from left to right. Dashed lines show symmetry lines used to minimize calculation domain. (B) Vertical flux calculated at different measuring heights along the line marked in panel A. For this surface heterogeneity (102 × 102 cm) and sediment surface roughness (1.32 cm), a fully integrated flux of 0.5 was first obtained for a measuring height of ~45 cm. (C – F) Two-dimensional flux distributions at each horizontal plane 5, 10, 15, and 45 cm above the sediment surface, respectively. Legend for panels A and C–F is located on the right.

dition ("inlet") was parameterized using values calculated at the downstream boundary ("outlet"), creating an infinite loop that allows the solution to run to steady state. An analytical solution to the one-dimensional formulation of the tracer release from a homogenous sediment surface was used as the initial conditions for the entire calculation domain to further minimize the total number of calculations to reach steady state. A wide range of field conditions were used in the simulations and are given in Table 1. These include 52 different pairs of sediment surface roughness (z_0) and friction velocity (u^*) calculated from the mean flow velocity at 15 cm above the bottom ($\bar{U}$) for each set of heterogeneity patch sizes (X), summing to a total of 276 separate steady state simulations

The numerical solution provided fluxes in three directions across the boundaries of all control volumes within the calculation domain. Distributions of vertical fluxes across the x and

Table 1. Input parameters used in model runs. $\bar{U}$ represents mean velocity at 15 cm above the benthic surface, z_0 represents sediment surface roughness, and u_* represents the friction velocity, calculated using a standard log-profile of flow (Stull 1988). X represents patch side length and width in centimeters. The model was run using all combinations of z_0, u_*, and X, adding up to a total of 276 and 52 seperate simulations for heterogeneity and response time, respectively.

	$\bar{U}$ (cm s^{-1})					
	1	**5**	**10**	**20**	**30**	**50**
z_0 (cm)			u_* (cm s^{-1})			
0.006	———	0.260	0.519	1.038	1.558	2.596
0.010	———	0.280	0.561	1.121	1.682	2.803
0.023	0.063	0.316	0.632	1.265	1.897	3.161
0.100	0.082	0.409	0.818	1.637	2.455	4.091
0.400	0.113	0.566	1.131	2.262	3.394	5.656
1.000	0.151	0.757	1.514	3.028	4.542	7.570
1.320	0.169	0.843	1.687	3.374	5.061	8.435
2.000	0.203	1.017	2.035	4.070	6.105	10.174
5.000	0.373	1.866	3.732	7.464	11.196	18.660
X (cm)	18	32	50	66	82	102

y direction (Fig. 2B) were used to determine the maximum variation of vertical fluxes from the average flux for each heterogeneous surface at different measuring heights. At a certain height above the lower boundary, which varied with z_0 and X, all variability vanished due to turbulent mixing and vertical fluxes for each control volume equaled the average vertical flux from the entire benthic surface. At this height and above, effects of individual bottom heterogeneities were no longer detectable and the vertical transport simplified to a 1D phenomenon. At heights below this threshold, vertical fluxes were not well integrated. By analyzing the results of each model simulation, threshold heights were identified where the vertical fluxes varied less than 5%, 10%, or 20% from the averaged benthic flux (h_5, h_{10}, and h_{20}).

Response time

The 90% response time (T_{90}) in EC measurements is defined as the time elapsed from when an abrupt change in benthic flux occurs until 90% of the change is registered at a given measuring height. The magnitude of T_{90} was examined using the 3D numerical model described above where all model parameters except the lower boundary condition were identical to those described previously. The lower boundary was defined as a uniform benthic surface with a flux that was abruptly increased from 0 to 1 at time zero. In each simulation the model was run until a steady state solution was reached. From each simulation, values of T_{90} were extracted at the measuring heights 5, 10, 15, 20, 30, and 45 cm above the sediment. Model runs were performed for the range of z_0 and u_* given in Table 1 for a total of 52 separate simulations.

Regression analysis

For each parameter tested, simple correlations were determined using a two-step regression analysis (Berg et al. 2007). For estimation of h_5, h_{10}, and h_{20}, the threshold heights were first correlated with z_0 and the coefficients from the initial fit were then correlated with X. T_{90} was initially correlated to u_* for each simulation based on a log-profile of flow (Stull 1988), and the coefficients were then correlated to the measuring height (h).

Example from Glud et al. (2010)

A site image and data from Glud et al. (2010) was used to give an example of the use of the correlations provided in this study. An image (station 4) from Glud et al. (2010) shows a heterogeneous site in a sub-arctic fjord located off the coast of Greenland with course sands interspersed with large rocks covered in calcareous algae. A characteristic heterogeneity patch size was determined by choosing 8 randomly distributed points on the image and measuring the horizontal lengths of the uniform benthic surface surrounding the points. As no information was available in Glud et al. (2010) on z_0, a sensitivity analysis was done using a range of roughness values that were 5%–30% of the characteristic patch size.

Assessment

Numerical solution

The numerical solution was tested to ensure assumptions based on minimizing the calculation domain as well as grid independence were fulfilled. Larger calculation domains were tested in the z-direction to ensure the calculation domain extended high enough in the water column so that the numerical solution was truly one-dimensional. Grid independence, defined as whether the numerical solution was impacted by reducing the control volume size, was also ensured for the standard control volume size of 2 cm × 2 cm in the x- and y-directions in additional simulations by using a finer control volume size of 1 cm × 1 cm, which gave the same result within 0.42%.

Heterogeneity

The modeled horizontal fields of the vertical flux were strongly correlated with sediment surface roughness (z_0), heterogeneity patch size (X), and measuring height (h). The example shown in Fig. 2 of one model run is based on X = 102 cm and z_0 = 1.32 cm. Figure 2C, D, E, and F show the vertical fluxes in the planes 5, 10, 15, and 45 cm above the bottom, respectively, illustrating that the heterogeneities in vertical fluxes are not fully integrated until 45 cm above the sediment surface. Wide ranges of z_0, X, and mean velocity ($\bar{U}$) were prescribed in model runs in order to simulate typical field conditions and can be found in Table 1. Similar to Berg et al. (2007), the vertical flux integration within the calculation domain was independent of $\bar{U}$.

As the distributions of the vertical flux were found to be independent of all variables other than z_0, X, and h, correlations for h_5, h_{10}, and h_{20} were determined in a two-step process where functions were fitted first to z_0 and then the coefficients of these functions were fitted to X. As an example, Fig. 3A shows all values of h_5 as a function of z_0 on a log axis (all $r^2 > 0.999$). The fitting function $h_5 = a + b(z_0)^c$ was used for all six different patch sizes tested. The coefficients were then fitted with the following functions and can be seen in Fig. 3B for h_5: $a = a_1 X + b_1$ and $b = a_2 X^{b2}$. The coefficient c was found to be constant for all correlations (Fig. 3B) of a given percent error (0.430, 0.458, and 0.487 for h_5, h_{10}, and h_{20}, respectively). This two-step process produced the following empirical relationships for the threshold measuring height with a user selectable maximum error of 5%, 10%, or 20%:

$$h_5 = 2.01X^{0.534} z_0^{0.430} + 0.0840X - 0.903 \quad (1)$$

$$h_{10} = 1.80X^{0.505} z_0^{0.458} + 0.0634X - 0.702 \quad (2)$$

$$h_{20} = 1.54X^{0.478} z_0^{0.487} + 0.0440X - 0.516 \quad (3)$$

where X is patch length in cm and z_0 is sediment surface roughness in cm. A visual test of the empirical relationships against the numerical solution is shown in Fig. 3C for h_5, and the average difference between the two solutions was found to be 0.4 ± 0.6, 0.8 ± 0.7, and 1.0 ± 0.8% for fits h_5, h_{10}, and h_{20}, respectively (SE, n = 52). The goodness of fit was tested statistically using a two sample Kolmogorov-Smirnov (K-S) test between the numerical model and the simple fits for each height (Massey 1951), and there were no significant differences between the numerical model and the simple fits (K-S stat = 0.0556, 0.0556, and 0.0370; P = 1.000 for Eqs. 1, 2, and 3, respectively).

Response time

An example of a simulated time series for a z_0 = 1.0 cm and $\bar{U}$ = 10 cm s^{-1} is given in Fig. 4, where the 90% response time (T_{90}) is generated as the time interval at which the flux

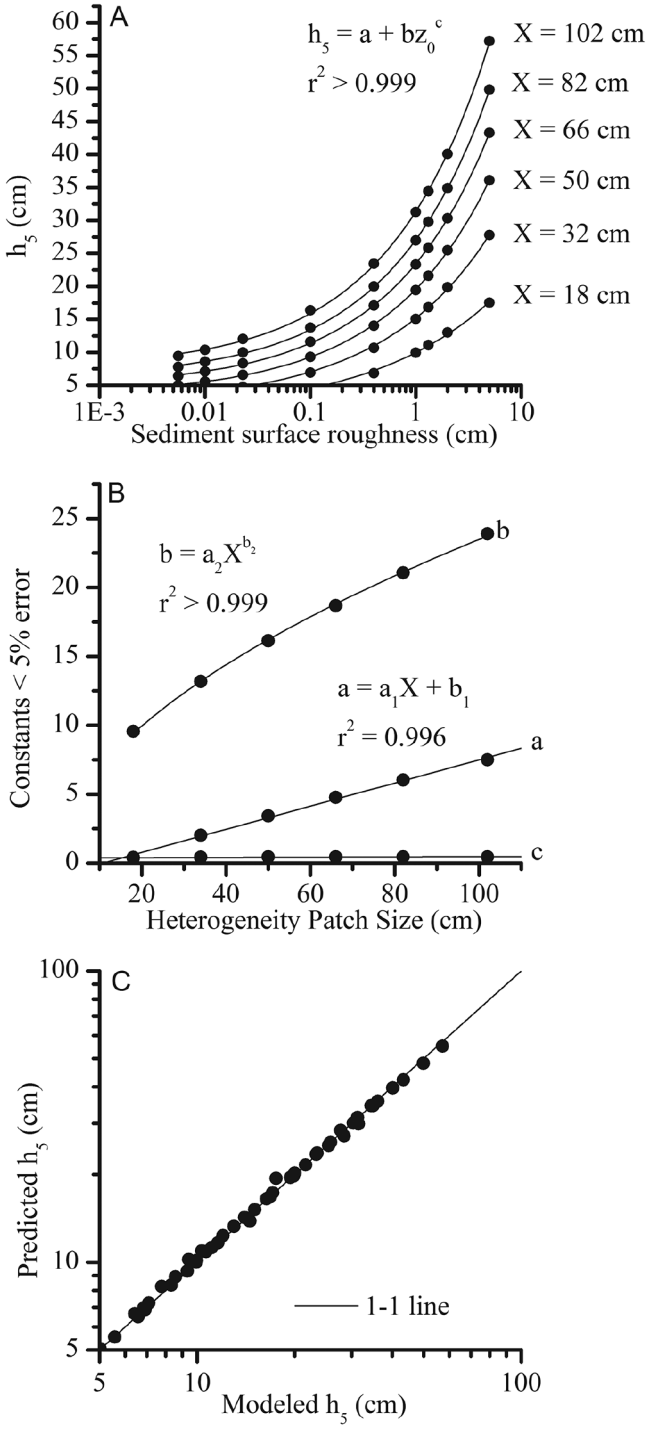

Fig. 3. (A) Minimum measuring height (h_5) required over a heterogeneous benthic surface to ensure < 5% error in flux measurements as a function of sediment surface roughness (z_0). Fits were generated using the curves from panel A and then the constants were used to fit with patch length to generate the final fits (Eqs. 1, 2, and 3). (B) Constants a and b fitted as a function of heterogeneity patch size (X). Constant c is given as the average value. (C) Predicted h_5 versus modeled h_5 shown with the 1-1 line. Predicted h_5 is not significantly different from modeled h_5 according to a two-sample Kolomogorov-Smirnov goodness of fit test (K-S stat = 0.556; P = 1.00).

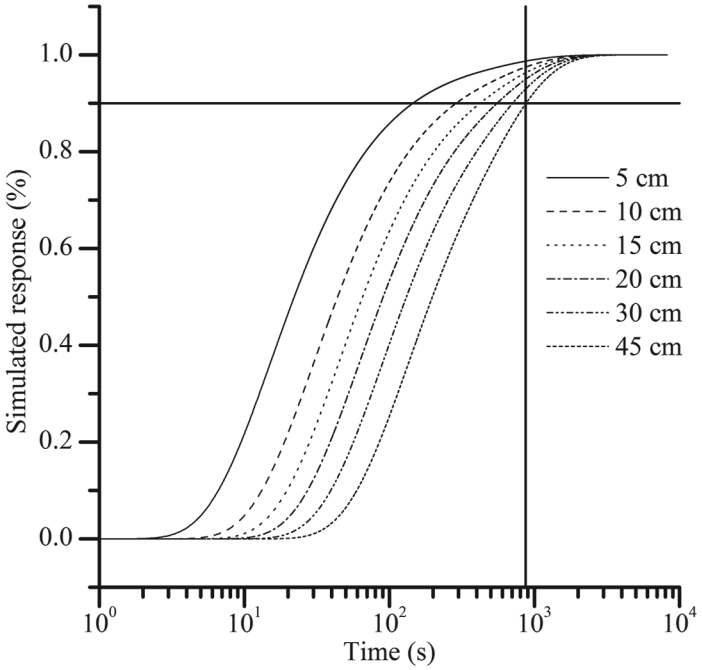

Fig. 4. Example model runs for 90% response time tests with z_0 = 0.1 cm and $\bar{U}$ = 10 cm s^{-1}. Timeseries was recorded at heights of 5, 10, 15, 20, 30, and 45 cm above the bottom after increasing the benthic flux from 0 to 1 at time zero and the horizontal line represents the 90% instrument response. Vertical line represents typical 870 seconds timeseries for calculation of one flux (Berg et al 2003).

reached 0.9 (from 0 at time zero) for each measuring height above the benthic surface. Values of T_{90} were found to be correlated with $\bar{U}$, z_0, and h. Through trial and error, it was found that the combined effect of z_0 and $\bar{U}$ can be merged into one variable, the friction velocity (u_*), defined as (Stull 1988):

$$u_* = \frac{\bar{U}\kappa}{\ln\left(\frac{h}{z_0}\right)} \quad (4)$$

where h is the measuring height above the bottom in cm, $\bar{U}$ is mean velocity at height h in cm s^{-1}, z_0 is sediment surface roughness in cm, and κ is Von Karmann's constant. Using a similar multi-step fitting process as previously described (Fig. 3 and 5A and B), a simple correlation was determined to estimate T_{90} as a function of u_* and h:

$$\log T_{90} = 2.87 - 1.22\left(0.92^{h}\right) - \log u_* \quad (5)$$

The average difference between the simple fit and the numerical solution was 1.3 ± 2.7% (SD, *n* = 324). The goodness of fit is shown in Fig. 5C and was tested statistically using a two sample K-S test (Massey 1951), and there was no significant difference between the two datasets (K-S stat = 0.0154, p = 1.00).

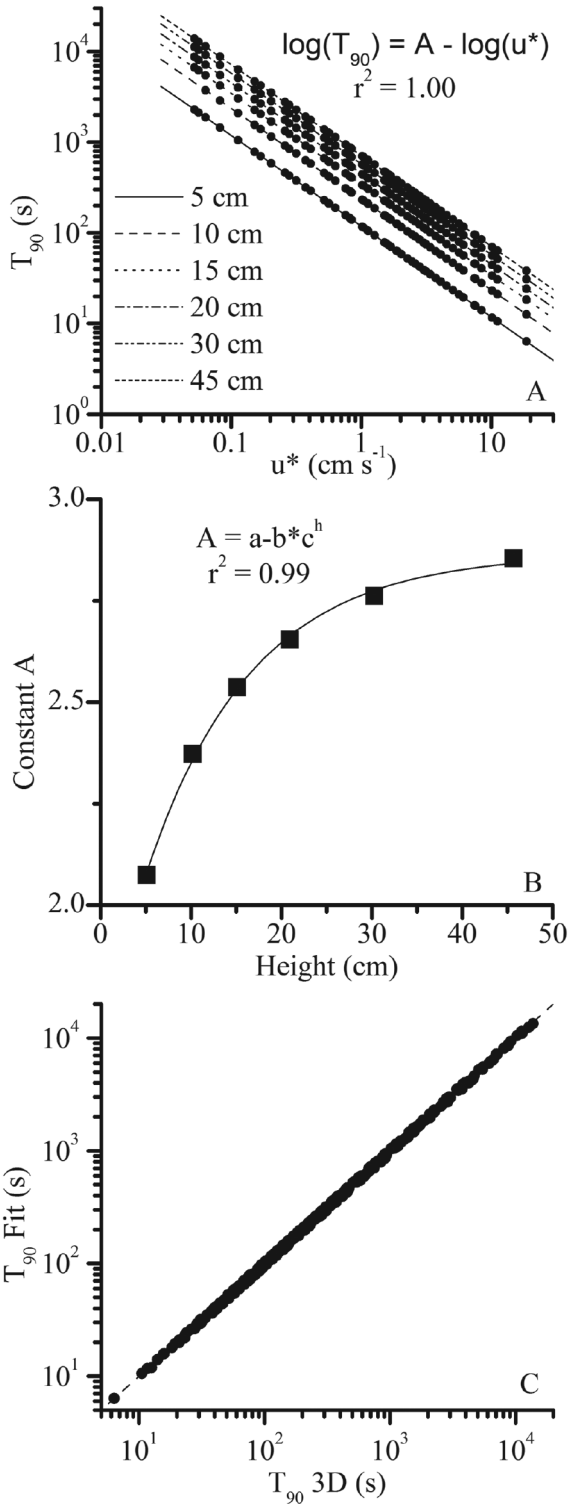

Fig. 5. (A) Fit of 90% response time (T_{90}) against friction velocity (Eq. 4, u_*) for different heights above the sediment surface. (B) Constant A fitted against measuring height to determine final fit (Eq. 5). (C) Simple fit plotted against the complex numerical model to show goodness of fit. Dashed line is the 1-1 line. A two sample K-S test showed no significant differences between the 3D model and the simple fit (K-S stat = 0.0154, p = 1.00, n = 324).

Example from Glud et al. 2010

The heterogeneity patch size (Station 4 in Glud et al. 2010) was determined to be 11 ± 2 cm (SE, n = 8). Using Eq. 1, 4, and 5, with z_0 defined from 0.5–3.0 cm, h_5 ranged from 5.5–11 cm, and T_{90} ranged from 4.3–11.5 min.

Discussion

This study reveals how aquatic EC measurements can be affected by heterogeneous benthic communities and temporal changes in the benthic flux. In determining ecosystem scale fluxes, these biases can be minimized if the set of simple guidelines derived in this study are followed when planning EC deployments and when the results are interpreted.

Generally, EC instruments are deployed above the roughness layer of the sediment surface and in the log layer of flow which typically extends up to 1 m above the seafloor (Boudreau and Jørgensen 2001). It is often assumed that with this approach, the footprint of the EC technique will be large enough to incorporate benthic heterogeneities and that the fluxes measured will be representative of the benthic community as a whole. However, this study shows that due to the uneven distribution of the flux signal within the footprint (Berg et al 2007), benthic fluxes measured in heterogeneous environments can be skewed toward one patch community type or another. For example, this could be significant if the site under study had patchy algal mats (e.g., Fig. 1) or a seagrass meadow with bare sediments interspersed. In these cases, if deployments were not properly planned to incorporate the benthic heterogeneity, biological interpretations of measured EC fluxes may differ depending on proximity of the instrument to one benthic patch community type or another.

The effect of heterogeneity was found to be correlated with heterogeneity patch size (X), measuring height (h), and sediment surface roughness (z_0). The effects of X and h are straightforward in that with larger patch sizes, more mixing is needed to integrate the flux signal well, requiring measurements higher above the sediment surface (e.g., Fig. 2). The effect of z_0 is more complex because z_0 changes the amount of turbulence in the flow (Stull 1988). Threshold values for h_5, h_{10}, and h_{20} increase with z_0 (Eq. 1, 2, and 3) because increased mixing associated with larger roughness elements make flux variations on the sediment surface penetrate higher in the water column. Thus, the effects of flux heterogeneity would be more pronounced, and the EC instrument would need to be deployed higher above the bottom to compensate.

The interpretation of EC fluxes in dynamic environments can be difficult due to non-steady state conditions (Holtappels et al. 2013). Data interpretation can be complicated by changes in O_2 concentration as well as current velocities (Holtappels et al. 2013), and we show that benthic flux variance in time can further impact EC data. Often, the controls on production or respiration, such as light or flow, can vary drastically over short periods of time (e.g., Hume et al. 2011). As these controlling variables may change on a time scale of minutes and the benthic community response may be nearly instantaneous, it is important to know how fast such changes are registered at the point where EC measurements are recorded. The 90% response time (T_{90}) is an estimate of the total time elapsed for 90% of a rapid change in benthic flux to reach the measuring height. Under extreme conditions for EC measurements (very high flows, rough sediment surfaces, and small measuring heights), T_{90} can be near instantaneous (~6 s, Fig. 5A); however, these field conditions are rare. Conventionally, many EC measurements have been recorded in 10–20 min bursts with individual flux estimates produced from each burst (Berg et al. 2003; Kuwae et al. 2006; Berg and Huettel 2008; Berg et al. 2009; Lorrai et al. 2010; Glud et al. 2010; McGinnis et al. 2011; Hume et al. 2011; Long et al. 2012; Reimers et al. 2012; Long et al. 2013; Berg et al. 2013). Under the majority of field conditions, with relatively rough sediment surfaces (e.g., z_0 = 0.01 cm) and middle range flow conditions (e.g., $\bar{U}$ = 5 cm s^{-1}), T_{90} was found to be shorter than this integration period. This suggests that interpretations of published EC fluxes are accurate with respect to this time lag. However, under some realistic field conditions (smooth sediment surfaces, low flows, and large measuring heights), T_{90} may be longer than the integration period of the EC data, indicating that this response time must be accounted for when dynamic fluxes are interpreted.

The parameters used in the correlations to determine the threshold measuring heights for h_5, h_{10}, and h_{20}, and T_{90} can be determined using several techniques. A simple field survey or image analysis can be used to determine X, the heterogeneity patch size. Values of z_0 and u* are more complex, but can be estimated using the high resolution EC data (Berg et al. 2007) where Reynold's stress and thus u* can be extracted from the 3D velocity field (*see* Berg et al. 2007).

The example with field data from Glud et al. (2010) illustrates how to use the derived correlations for measuring heights that ensure appropriate integration of fluxes from heterogeneous sediments (Eq. 1) and to estimate T_{90} (Eq. 4, 5). The heterogeneity patch size was estimated from a photograph to be 11 ± 2 cm (SE, n = 8), $\bar{U}$ was given by Glud et al. (2010) to be ~2 cm s^{-1}, and z_0 was assumed to range from 0.5–3.0 cm, as no data for this parameter were available. Using Eq. 1, 4, and 5, h_5 ranged from 5.5–11 cm, and T_{90} ranged from 4.3–11.5 min. These first order estimates suggest that regardless of the roughness chosen for the site, the measuring height used by Glud et al. (2010) (h = 8-10 cm) was high enough above the benthic surface to incorporate heterogeneous fluxes appropriately into their measurements. Also, for the range of z_0 used in this estimate, T_{90} for their study site was well within the length of a single flux calculation (T_{90} < 14.5 min), indicating that most of a sudden change in benthic flux would be incorporated into the relevant flux estimate.

In this study, and in the earlier footprint study by Berg et al. (2007), unidirectional current flow was assumed in all calculations and the presence of surface waves was considered negligible. However, in many cases, significant wave action

has been found at shallower sites where the EC technique has been applied (Berg and Huettel 2008; Reimers et al. 2012; Long et al. 2013). The effects of wave action on the footprint, the technique's ability to integrate over heterogeneous surfaces, and the 90% response time should be included in future modeling studies to further improve the interpretation and understanding of aquatic EC measurements.

Comments and recommendations

This modeling study represents a simplistic approach to determining the effects of spatial and temporal variability at the sediment surface on aquatic eddy correlation flux measurements. Whereas we realize that the ideal conditions that must be assumed in a mechanistic modeling exercise do not always exist in natural field situations, the derived simple correlations still provide guidance in preparation of EC deployments and interpretation of EC data. Specifically, we recommend using these equations to select appropriate measuring heights for a given study site. However, the equations for h_s, h_{10}, and h_{20} will provide measuring heights that may not be ideal or possible, such as very close to the sediment surface (i.e., 5 cm or below) where we would not recommend attempting deployments. We also recommend using the equations to determine T_{90} when dynamic fluxes EC data are interpreted. Site selection and deployment planning are important components of using the EC technique, and at sites that are heterogeneous, this study shows that there may be a tradeoff between a fast response time and a full integration of heterogeneous fluxes to estimate an ecosystem scale fluxes.

References

Berg, P., H. Roy, F. Janssen, V. Meyer, B. B. Jørgensen, M. Huettel, and D. de Beer. 2003. Oxygen uptake by aquatic sediments measured with a novel non-invasive eddy-correlation technique. Mar. Ecol. Prog. Ser. 261:75-83 [doi:10.3354/meps261075].

———, H. Roy, and P. L. Wiberg. 2007. Eddy correlation flux measurements: The sediment surface area that contributes to the flux. Limnol. Oceanogr. 52(4):1672-1684 [doi:10.4319/lo.2007.52.4.1672].

———, and M. Huettel. 2008. Monitoring the seafloor using the noninvasive eddy correlation technique: Integrated benthic exchange dynamics. Oceanography 21(4):164-167 [doi:10.5670/oceanog.2008.13].

———, R. N. Glud, A. Hume, H. Stahl, K. Oguri, V. Meyer, and H. Kitazato. 2009. Eddy correlation measurements of oxygen uptake in deep ocean sediments. Limnol. Oceanogr: Methods 7:576-584 [doi:10.4319/lom.2009.7.576].

———, and others. 2013. Eddy correlation measurements of oxygen fluxes in permeable sediments exposed to varying current flow and light. Limnol. Oceanogr. 58(4):1329-1343. [doi:10.4319/lo.2013.58.4.1329].

Boudreau, B. P., and B. B. Jørgensen. 2001. The benthic boundary layer: transport processes and biogeochemistry. Oxford Univ. Press.

Brand, A., D. F. McGinnis, B. Wehrli, and A. Wuest. 2008. Intermittent oxygen flux from the interior into the bottom boundary of lakes as observed by eddy correlation. Limnol. Oceanogr. 53(5):1997-2006 [doi:10.4319/lo.2008.53.5.1997].

Carnahan, B., H. A. Luther, and J. O. Wilkes. 1969. Applied numerical methods. Wiley.

Douglas, J. 1955. On the numerical integration of $\partial^2u/\partial x^2 + \partial^2u/\partial y^2 = \partial u/\partial t$ by implicit methods. J. Soc. Indust. Appl. Math. 3:42-65.

Glud, R. N., P. Berg, A. Hume, P. Batty, M. E. Blicher, K. Lennert, and S. Rysgaard. 2010. Benthic O_2 exchange across hard bottom substrates quantified by eddy correlation in a sub-Arctic fjord. Mar. Ecol. Prog. Ser. 417:1-12 [doi:10.3354/meps08795].

Holtappels, M., R. N. Glud, D. Donis, B. Liu, A. Hume, F. Wenzh?fer, and M. M. M. Kuypers. 2013. Effects of transient bottom water currents and oxygen concentrations on benthic exchange rates as assessed by eddy correlation measurements. J. Geophys. Res. Oceans 118:1-13 [doi:10.1002/jgrc.20112].

Hume, A., P. Berg, and K. McGlathery. 2011. Dissolved oxygen fluxes and ecosystem metabolism in an eelgrass (*Zostera marina*) meadow measured with the eddy correlation technique. Limnol. Oceanogr. 56(1):86-96 [doi:10.4319/lo.2011.56.1.0086].

Kuwae, T., K. Kamio, T. Inoue, E. Miyoshi, and Y. Uchiyama. 2006. Oxygen exchange flux between sediment and water in an intertidal sandflat, measured in situ by the eddy-correlation method. Mar. Ecol. Prog. Ser. 307:59-68 [doi:10.3354/meps307059].

Long, M. H., D. Koopmans, P. Berg, S. Rysgaard, R. N. Glud, and D. H Sogaard. 2012. Oxygen exchange and ice melt measured at the ice-water interface by eddy correlation. Biogeosciences 9(6):1957-1967 [doi:10.5194/bg-9-1957-2012].

———, P. Berg, D. de Beer, and J. Zieman. 2013. In situ coral reef oxygen metabolism: an eddy correlation study. PloS ONE 8(3):e58581 [doi:10.1371/journal.pone.0058581].

Lorrai, C., D. F. McGinnis, A. Brand, and A. Wuest. 2010. Application of oxygen eddy correlation in aquatic systems. J. Atmos. Ocean. Tech. 27:1533-1546 [doi:10.1175/2010JTECHO723.1].

Massey, F. J. 1951. The kolmogorov-smirnov test for goodness of fit. J. Amer. Stat. Assoc. 46(253):68-78 [doi:10.1080/01621459.1951.10500769].

McGinnis, D. F., P. Berg, A. Brand, C. Lorrai, T. J. Edmonds, and A. Wüest. 2008. Measurements of eddy correlation oxygen fluxes in shallow freshwaters: Towards routine applications and analysis. Geophys. Res. Lett. 35:L04403 [doi:10.1029/2007GL032747].

———, and others. 2011. Simple, robust eddy correlation amplifier for aquatic dissolved oxygen and hydrogen sulfide flux measurements. Limnol. Oceanogr. Methods. 9:340-347 [doi:10.4319/lom.2011.9.340].

Peaceman, D. W., and H. H. Rachford. 1955. The numerical solution of parabolic end elliptic differential equations. J. Soc. Indust. Appl. Math. 3:28-41 [doi:10.1137/0103003].

Reimers, C. E., H. T. Ozkan-Haller, P. Berg, A. Devol, K. McCann-Grosvenor, and R. D. Sanders. 2012. Benthic oxygen consumption rates during hypoxic conditions on the Oregon continental shelf: Evaluation of the eddy correlation method. J. Geophys. Res. 117:1-18 [doi:10.1029/2011JC007564].

Stull. R. B. 1988. The mathematical theory of turbulence. Springer-Verlag.

Swinbank, W. C. 1951. The measurement of vertical transfer of heat and water vapor by eddies in the lower atmosphere. J. Meteor. 8(3):135-145 [doi:10.1175/1520-0469(1951)008<0135:TMOVTO>2.0.CO;2].

Submitted 19 December 2012
Revised 26 April 2013
Accepted 1 June 2013